Available online at www.sciencedirect.com

ScienceDirect

Ceramics International 39 (2013) 8605–8614

CERAMICS INTERNATIONAL

www.elsevier.com/locate/ceramint

# Domain texture dependent fracture behavior in mechanically poled/depoled ferroelectric ceramics

Yingwei Li[a], Yao Sun[a], Faxin Li[a,b,*]

[a]State Key Lab for Turbulence and Complex Systems, College of Engineering, Peking University, Beijing 100871, China
[b]HEDPS, Center for Applied Physics and Technologies, Peking University, Beijing, China

Received 11 February 2013; received in revised form 28 March 2013; accepted 6 April 2013
Available online 18 April 2013

## Abstract

The influence of domain texture on the fracture behavior was investigated in both the mechanically poled (MP) and the mechanically depoled (MD) PZT ceramics. Firstly, we fabricated axisymmetric domain textures in the MP and MD PZT samples subjected to a series of compressive stresses of up to 400 MPa. Then the Vickers indentation was employed to measure the fracture toughness parallel to ($K_{IC}^{\parallel}$) and perpendicular to ($K_{IC}^{\perp}$) the compression direction. Results show that with increasing compressive stress, $K_{IC}^{\perp}$ increases and $K_{IC}^{\parallel}$ decreases in both the MP and MD samples and $K_{IC}^{\perp}$ can reach 2.6–2.7 MPa m$^{1/2}$ at 400 MPa. Such fracture behavior is attributed to the ferroelastic domain switching toughening mechanism in ferroelectric ceramics, and the fracture toughness is proportional to the texture-dependent switchable strain near the crack surface. The obtained results may provide a helpful guidance for improving the reliability and performance of ferroelectric capacitors.


*Keywords:* Domain texture; Fracture toughness; Ferroelectric ceramics; Domain switching

## 1. Introduction

As the “smartest” materials, ferroelectric materials have been widely used in modern industries as capacitors, sensors, actuators, etc. due to their high permittivity, peculiar electromechanical properties, and compact size [1,2]. However, because ferroelectric ceramics are very brittle, the fracture problem during operation has severely limited their applications in high reliable devices [3,4]. In order to improve the reliability and extend the lifetime of ferroelectric devices, it is essential to investigate the fracture behavior of ferroelectric ceramics.

During the past decades, intensively experimental works [5–8] as well as theoretical [9,10] studies have been conducted to address the fracture behavior of ferroelectric ceramics. Although debates still exist for some problems [3,4], such as the influence of electric fields on the fracture toughness, it has been widely accepted that domain switching plays an important role in crack propagation [3–10]. Typically, there are two physical mechanisms leading to domain reorientation near the crack surface: one is the Lehovec effect [11], and the other is ferroelastic domain switching caused by the singular stress fields near the crack tip [5–10]. The Lehovec effect means that a very large depolarization field exists within a thin layer just beneath the surface of ferroelectric materials, tending to orient the polar axes of ferroelectric domains perpendicular to the crack surface [11]. As domain switching always dissipates energy, ferroelectric materials usually show fracture toughness enhancement during crack propagation, exhibited as R-curves [5–7]. Furthermore, as the amount of the switchable domains near the crack surface is texture dependent, ferroelectric materials will show fracture toughness anisotropy (FTA) in the pre-poled specimens [12].

The FTA phenomenon in ferroelectric ceramics was first discovered by Okazaki and co-workers in early 1980s [12]. When they used the indentation method to measure the fracture toughness of the unpoled and/or electrically poled $PbTiO_3$ and PLZT ceramics, they found that the crack lengths were the same in the unpoled samples but different in the poled samples, i.e., the crack parallel to the poling direction (hereafter referred as parallel crack) is shorter than that perpendicular to (hereafter referred as vertical crack) it. Anisotropic

*Corresponding author at: State Key Lab for Turbulence and Complex Systems, College of Engineering, Peking University, Beijing 100871, China. Tel.: +86 10 62757454; fax: +86 10 62751812.
*E-mail addresses:* lifaxin@pku.edu.cn, lifaxin@coe.pku.edu.cn (F. Li).

0272-8842/$ - see front matter © 2013 Elsevier Ltd and Techna Group S.r.l. All rights reserved.
http://dx.doi.org/10.1016/j.ceramint.2013.04.034

residual internal stress generated during electric poling was suggested to account for the observed FTA. Latter, Pisarenko et al. [13] systematically investigated the FTA in PZT and barium titanate ceramics by using double torsion and indentation methods. They thought the FTA was mainly caused by texture-dependent domain reorientation near the crack tip. In 1990, Mehta and Virkar [14] verified the domain switching toughening mechanism by measuring the domain textures beneath the crack surface using X-ray diffraction. In addition, they found FTA in the unpoled samples after mechanical poling (mechanical poling means that reorienting the domains in an unpoled sample by using a large uni-axial compressive stress. If the unpoled sample is replaced by a poled sample, then the process is called mechanical depoling). This phenomenon was attributed to the anisotropic domain textures after compression. Later the fracture behavior of electrically poled samples had been investigated by Guiu et al. [15], Calderon-Moreno and Popa [16], Fang and Yang [17], dos Santos e Lucato et al. [6], etc. using indentation, three point bending and compact tension methods. It is found that the fracture toughness measured by different methods can qualitatively confirm with each other. However, the FTA ratio measured by the indentation method is larger than that by other methods [16,17]. Recently, a large FTA ratio of 3.82 was found in the mechanically poled PZT samples by Li and Li [18], and they attributed this to that the domain textures in the mechanically poled samples are more saturated than that in the electrically poled samples. So far, studies on the fracture behavior of ferroelectric ceramics have been focused on the electrically poled samples; while the mechanically poled (MP) samples had little been concerned [14,18]. The MP ferroelectric ceramics, although cannot be used in piezoelectric applications, may have special applications in high reliable capacitor areas because of their large fracture toughness perpendicular to the loading direction, and should be intensively studied.

In this paper, the fracture behavior of the partial/complete mechanically poled/depoled Lead Titanate Ziconate (PZT) ceramics was systematically investigated using the Vickers indentation method. The longitudinal strains during mechanical poling/depoling were monitored by strain gauges and the domain textures were characterized by X-ray diffraction. The Vickers indentation results show that in both types of PZT samples, the fracture toughness perpendicular to the loading direction increases and that parallel to it decreases with increasing compressive stress. The domain texture dependent fracture toughness is thought to be caused by the ferroelastic domain switching toughening mechanism in ferroelectric ceramics.

## 2. Experimental procedure

### 2.1. Specimen preparation

The material used in this study is soft PZT ceramics, provided by Institute of Acoustics, Chinese Academy of Sciences. Its composition is near the morphtropic phase boundary where the Zr/Ti ratio is at 52/48. Its Curie temperature is at 315.2 °C. The material is cut into blocks with dimension of $6 \times 6 \times 12\ \mathrm{mm}^3$. Silver paste is sintered onto the two opposite $6 \times 6\ \mathrm{mm}^2$ surfaces of the blocks as electrodes. Electrical poling is conducted above the Curie point using a DC electric field of 500 V/mm along the 12 mm direction. The sample is then gradually cooled to room temperature with the electric field on. After poling, the piezoelectric constant $d_{33}$ was measured to be $495 \pm 8$ pC/N.

### 2.2. Mechanical poling/depoling and texture measurement

The testing setup for the mechanical poling/depoling is shown in Fig. 1. The compressive stress is applied to the specimen by a screw-driven testing machine (Shimadzu, Japan), together with a spherical hinge to avoid any bias compression. Strain gauges are glued on the two opposite $6 \times 12\ \mathrm{mm}^2$ surfaces to measure the variations of longitudinal strain during compression. Two pieces of copper wafer are pressed to the sample as electrodes and two alumina blocks are used as insulators to separate the testing machine from the high-voltage loading. The charges released during depolarization is collected by a capacitor of 10 μF and measured by a charge amplifier connected in series. During testing, the signals of stress, strain and the charges are input into an A/D data acquisition card and monitored by a computer.

Before testing, the edges of the specimen were polished to avoid stress concentration during testing. The specimen was then put on the center of the loading equipment and a preload of about 18 N was used to fix it. The strain signals of the two strain gauges are used to adjust the specimen to realize the uniaxial compression without bending. The compression loading rate is set to be 5 MPa/s and unloading starts as soon as the maximum compression reached, at a rate of about 10 MPa/s. For mechanical poling, the compressive stress levels of 50 MPa, 100 MPa, 200 MPa, and 400 MPa were used. As for mechanical depoling, a series of stresses of 50 MPa, 60 MPa, 70 MPa, 80 MPa, 100 MPa, 200 MPa, and 400 MPa were used to capture the point where the fracture toughness anisotropy switches.

After mechanical poling/depoling, X-ray diffraction was explored to detect the domain textures of the samples on the

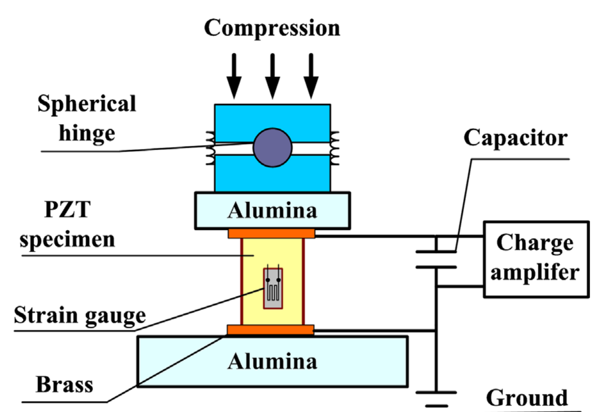


Fig. 1. Testing setup for the mechanical poling/depoling of ferroelectric ceramics.

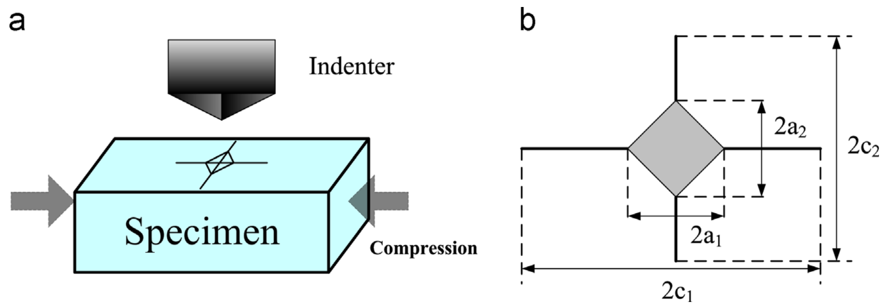


Fig. 2. (a) Illustration of the Vickers indentation method and (b) the measured parameters after indentation.

surface perpendicular to the compression direction. A Philips X'PertPro powder diffractometer was employed using CuKα radiation with the wavelength of $\lambda = 1.54046$ Å and the $2\theta$ angle resolution of 0.001°. The diffraction angle $2\theta$ is scanned from 42° to 47° with a speed of 0.5°/min.

### 2.3. Fracture toughness measurement

For all the mechanical poled/depoled samples, a $6 \times 12$ mm$^2$ face was polished with 0.5 μm diamond polishing solution, and cleaned in acetone by a supersonic cleaner for 1 min. The Vickers indentation was then made on the polished surfaces using a fixed load of 19.8 N, with the holding time of 10 s. The two diagonals of the indentation were aligned parallel and perpendicular to the compression directions (Fig. 2(a)). For each sample, 10 Vickers indention points were conducted on the polished surface. The lengths of $a_1$ and $a_2$ were measured for the calculation of the hardness, and $c_1$ and $c_2$ were measured to calculate the fracture toughness of the sample, as shown in Fig. 2(b). For comparison, the fracture toughness of the unpoled and electrically poled samples was also measured.

## 3. Results and discussions

### 3.1. Mechanical poling/depoling

Fig. 3 shows the measured stress–strain curves of the unpoled PZT samples during uni-axial compression loading/unloading with different levels of applied stresses. It can be seen that all the samples shrink along the compression direction and show significant nonlinear behavior, indicating that some domains switch their polar directions to the plane perpendicular to the compression [19]. As ferroelastic domain switching can occur at a very low stress, a distinct coercive stress cannot be distinguished from Fig. 3. Meanwhile, it can be seen that both the maximum strain and the remnant strain increase steadily with increasing stress, i.e., more domains can accomplish ferroelastic switching at higher stresses. When the stress is above 350 MPa, the ferroelastic domain switching is nearly saturated and the strain–stress curve is almost linear from 350 MPa to 400 MPa. During stress unloading, all the curves are firstly linear and then show nonlinear behavior, indicating that the vanishing applied stress cannot balance the internal stress caused by ferroelastic domain switching thus some domains switched back to their unpoled states [20].

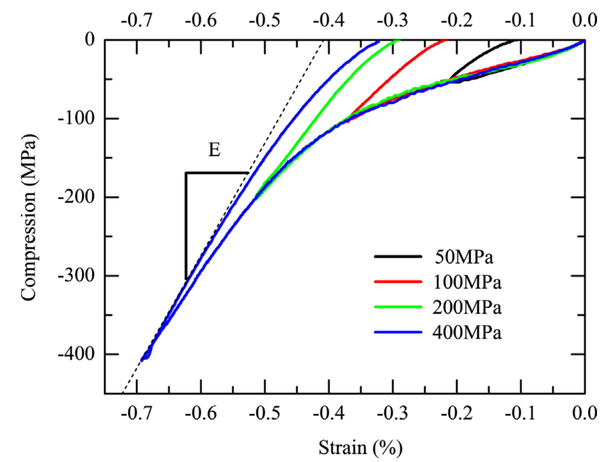


Fig. 3. Stress–strain curves of the unpoled PZT samples during mechanical depoling with different levels of stress.

Similarly, the electrically poled PZT samples during mechanical depoling show the similar stress–strain curves with the unpoled specimens, as shown in Fig. 4(a). However, at the same level of stress, both the maximum strain and the remnant strain of the depoled samples are larger than that of the mechanically poled samples. This is due to that in the electrically poled PZT samples, the polar axes of domains had been oriented by the large poling field along the 12 mm direction. Hence more domains can switch during compression along the poling direction. In addition, as the space charges cannot be balanced by the remnant polarization any longer after domain reorientation, these charges are released and turn to be free charges. They will move onto the electrodes and then the samples show stress–depolarization curves, as shown in Fig. 4(b).

Fig. 5 shows the relationship between the remnant strains and the applied compressive stress. For comparison, the sum of the remnant strain (0.32%) for the electrically poled samples and the remnant strains of the MP samples were plotted together in Fig. 5. It can be seen that for both the MP and MD samples, the remnant strain varies significantly with the stress below 200 MPa, indicating that domain reorientation occurs mainly in this stress range. When the stress increases from 200 MPa to 400 MPa, the remnant strains of the MP and MD samples increase only 0.03% and 0.09%, respectively. Under

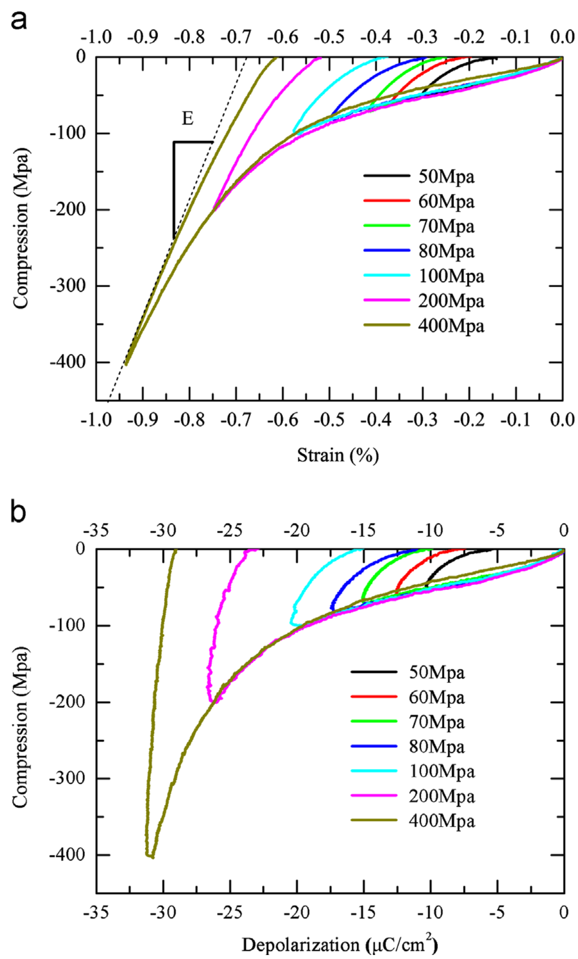


Fig. 4. Stress–strain curves (a) and stress–depolarization curves (b) of the electrically poled PZT samples during mechanical depolarization with different levels of applied stresses.

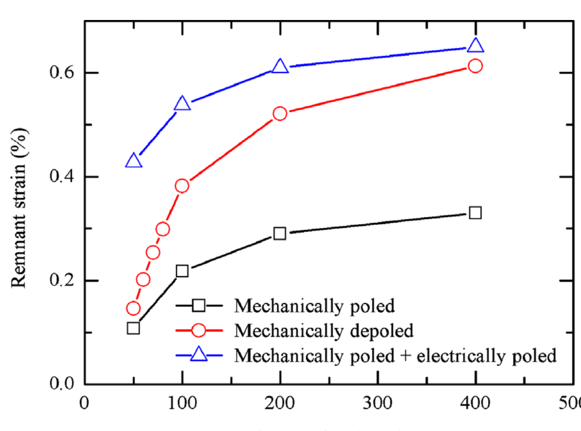


Fig. 5. The remnant strain vs. compressive stress of the MP and MD PZT samples.

the maximum compression of 400 MPa, the measured remnant strain of the MP sample can reach 0.33%, slightly larger than that of 0.32% after electric poling. However, previous studies have shown that the theoretically saturated remnant strain in an electrically poled ferroelectric ceramics is larger than that in a compression poled one, with the ratio of the former to the latter being 1.37 for the tetragonal ceramics and 1.48 for the rhombohedral [21]. Therefore, the mechanically poled PZT ceramics are closer to the theoretically saturated state than the electrically poled one. It can be seen from Fig. 5 that the remnant strains of the mechanically depoled samples are always smaller than the sum of remnant strains of the MP samples and the electrically poled samples, indicating the domain textures of the MP samples are more saturated than those of the MD samples at the same level of stress, even when the compressive stress reach up to 400 MPa.

Fig. 6 shows the X-ray diffraction results of the MP and MD PZT samples. It can be seen clearly that for both types of samples, the ratio of the 002 peak to 200 peak of the tetragonal phase, i.e., $I^T_{002}/I^T_{200}$, increases steadily with increasing compressive stress, which confirms that the larger the stress is, the more domains can switch with their elongation axis as close as possible to the plane perpendicular to the loading direction. Moreover, by comparing the XRD data of the MP samples and MD samples at the same stress, it can be seen that the $I^T_{002}/I^T_{200}$ ratio of the former is larger than that of the latter, which further verified that domain textures in the MP sample is more saturated than that in the MD samples at the same level of compression. Due to the overlap of intensity peaks of the tetragonal phase and the

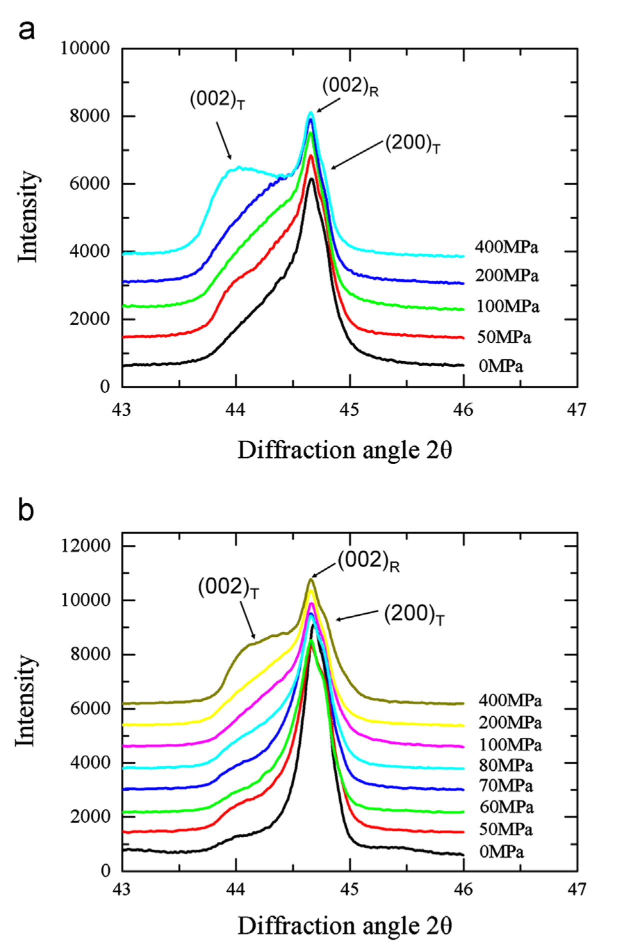


Fig. 6. X-ray diffraction results of the mechanically poled samples (a) and the mechanically depoled samples (b).

rhombohedral phase, the possible phase transformation during compression, and the possible existing monoclinic phase [22], the precision texture cannot be extracted from the XRD results.

### *3.2. Fracture toughness of the mechanically poled/depoled samples*

Fig. 7(a)–(d) shows the photographs of the microindents of the unploed, mechanically poled (400 MPa), electrically poled, and mechanical depoled (400 MPa) PZT samples. For the unpoled sample, the length of cracks along the two diagonals of the indentation is nearly equal, as shown in Fig. 7(a). After mechanical poling, the parallel crack increases but the perpendicular crack decreases, thus the sample exhibits fracture toughness anisotropy (FTA), as shown in Fig. 7(b). As to the electrically poled PZT in Fig.7(c) where the domain textures had been oriented by applied electric field, the parallel cracks are shorter than the perpendicular cracks which are quite different from that in the MP samples. After mechanical depoling by a stress of 400 MPa, the parallel cracks turn to be longer than the perpendicular cracks, and the sample shows similar FTA with the MP samples, as shown in Fig. 7(d).

The measured crack lengths and Vickers Hardness of all the MP and MD samples at different levels of compression are listed in Table 1. Then, their fracture toughness is calculated using the following well known expression [23]:

$$K_{IC} = k(E/\mathrm{Hv})^{1/2} P/c^{3/2} \tag{1}$$

where $E$ and Hv are Young's modulus and Vickers hardness, respectively and $k$ is a dimensionless constant, usually takes the value of $0.016 \pm 0.004$, suggested by Anstis et al. [23]. In calculation, Young's modulus $E$ measured from the 400 MPa mechanical poling and depoling curves was used for MP and MD samples, respectively (this is because $E$ measured from the 400 MPa stress–strain curves is though to be the "true" Young's modulus of these materials [24]).

The calculated fracture toughness of the MP and MD samples are shown in Fig. 8. It can be seen that for both types of samples, with increasing compressive stress, the fracture toughness perpendicular to the loading direction ($K_{IC}^{\perp}$) increases and the fracture toughness along the loading direction ($K_{IC}^{\parallel}$) decreases. For the unpoled samples, the fracture toughness is isotropic, with the average value of $1.08 \pm 0.06$ MPa m$^{1/2}$. After mechanical poling by a maximum stress of 400 MPa, $K_{IC}^{\perp}$ reaches 2.7 MPa m$^{1/2}$ and

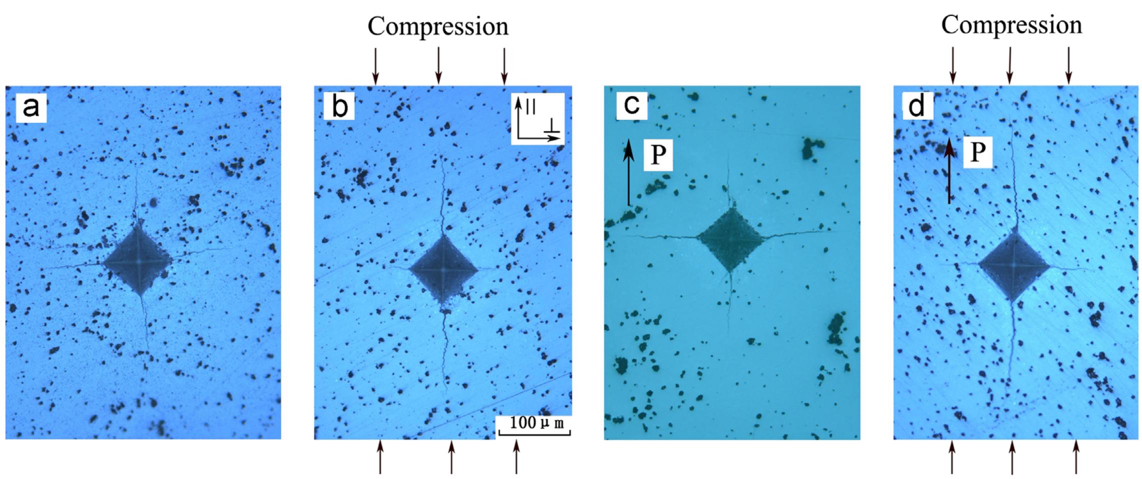


Fig. 7. Photographs of the microindents in (a) unpoled, (b) mechanically poled (400 MPa), (c) electrically poled, and (d) mechanically depoled (400 MPa) PZT samples. P denotes the electric poling direction.

Table 1
The crack length and Vickers hardness for the mechanically poled/depoled PZT specimen after different levels of compression.

| Compression stress (MPa) | Mechanically poled | | | Mechanically depold | | |
|---|---|---|---|---|---|---|
| | Hv (GPa) | Crack length (μm) | | Hv (GPa) | Crack length (μm) | |
| | | Perpendicular | Parallel | | Perpendicular | Parallel |
| 0 | $3.395 \pm 0.054$ | $295.6 \pm 11.6$ | | $3.337 \pm 0.115$ | $429.8 \pm 7.8$ | $226.4 \pm 6.0$ |
| 50 | $3.555 \pm 0.107$ | $220.4 \pm 20.5$ | $348.2 \pm 18.4$ | $3.067 \pm 0.204$ | $410.1 \pm 38.1$ | $228.9 \pm 11.8$ |
| 60 | – | – | – | $2.823 \pm 0.182$ | $420.5 \pm 18.2$ | $274.4 \pm 16.0$ |
| 70 | – | – | – | $2.620 \pm 0.209$ | $319.0 \pm 16.8$ | $306.4 \pm 24.6$ |
| 80 | – | – | – | $2.843 \pm 0.145$ | $260.4 \pm 18.0$ | $374.5 \pm 12.4$ |
| 100 | $3.516 \pm 0.056$ | $181.1 \pm 11.5$ | $364.0 \pm 13.9$ | $2.924 \pm 0.195$ | $185.5 \pm 10.6$ | $345.9 \pm 18.9$ |
| 200 | $3.539 \pm 0.093$ | $164.3 \pm 8.3$ | $367.1 \pm 18.0$ | $3.570 \pm 0.081$ | $170 \pm 11.2$ | $356.3 \pm 10.7$ |
| 400 | $3.581 \pm 0.101$ | $154.9 \pm 7.7$ | $370.6 \pm 19.3$ | $3.562 \pm 0.099$ | $161.5 \pm 4.5$ | $370.2 \pm 13.7$ |

$K_{IC}^{\parallel}$ deceases to 0.75 MPa m$^{1/2}$, with the fraction toughness anisotropy ratio ($K_{IC}^{\perp}/K_{IC}^{\parallel}$) of 3.7. For the electrically poled samples, $K_{IC}^{\parallel}$ is larger than $K_{IC}^{\perp}$, with the anisotropy ratio ($K_{IC}^{\perp}/K_{IC}^{\parallel}$) of 1/2.6. When the depoling stress reaches about 70 MPa, the fracture toughness of the MD sample turns to be isotropic, with the average value of 1.2 MPa m$^{1/2}$, slightly larger than that of the unpoled samples. When the depoling stress is larger than 70 MPa, $K_{IC}^{\perp}$ turns to be larger than $K_{IC}^{\parallel}$ and the MD samples show anisotropic fracture toughness again. When the depoling stress reaches its maximum value of 400 MPa, $K_{IC}^{\perp}$ increases to 2.6 MPa m$^{1/2}$ and $K_{IC}^{\parallel}$ deceases to 0.75 MPa m$^{1/2}$, with the anisotropy ratio ($K_{IC}^{\perp}/K_{IC}^{\parallel}$) of 3.5, slightly smaller than 3.7 in the MP sample at 400 MPa, which is consistent with that of the domain textures in the MD samples which are not so saturated as that in the MP samples.

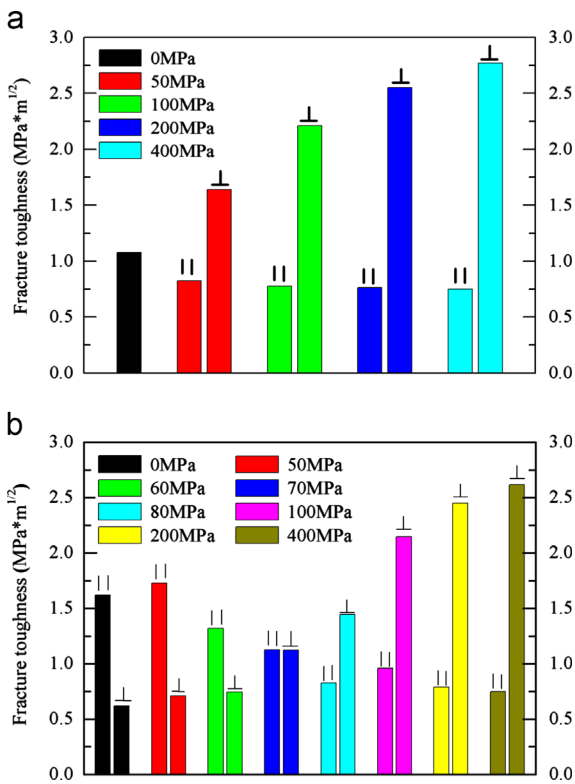


Fig. 8. The fracture toughness of the mechanically poled (a) and mechanically depoled (b) PZT samples after different levels of compression.

The fracture toughness anisotropy in the electrically poled ferroelectric ceramics had been explained by the domain switching induced toughening mechanism [5–10,13–18], which should also account for the observed FTA in the MP and MD PZT samples in this work. The fracture toughness of ferroelectric material can be divided into two parts: one is the "intrinsic" fracture toughness without the influence of domain switching; the other is the enhancement of fracture toughness induced by domain switching. From the energy point of view, the critical energy release rate (ERR) of ferroelectric ceramics can also be split into two parts as

$$G_{IC} = G_0 + \Delta G_{IC} \tag{2}$$

where $G_{IC}$ represent the critical ERR during crack growth; $G_0$ denotes the intrinsic critical ERR without domain switching; and $\Delta G_{IC}$ is the enhancement of the critical ERR caused by domain switching.

In the unpoled sample, the polarization directions of domains are randomly distributed, as shown in Fig. 9(b). Because of the Lehovec effect and tensile stress near the crack tip [7,8,11], domains will always orient with their polar axes perpendicular to the crack surface. Therefore, when the Vickers indentation is applied onto an unpoled sample, the domain textures on the crack surfaces will change from Fig. 9 (b) to (c) and (d) for the parallel crack and perpendicular crack,

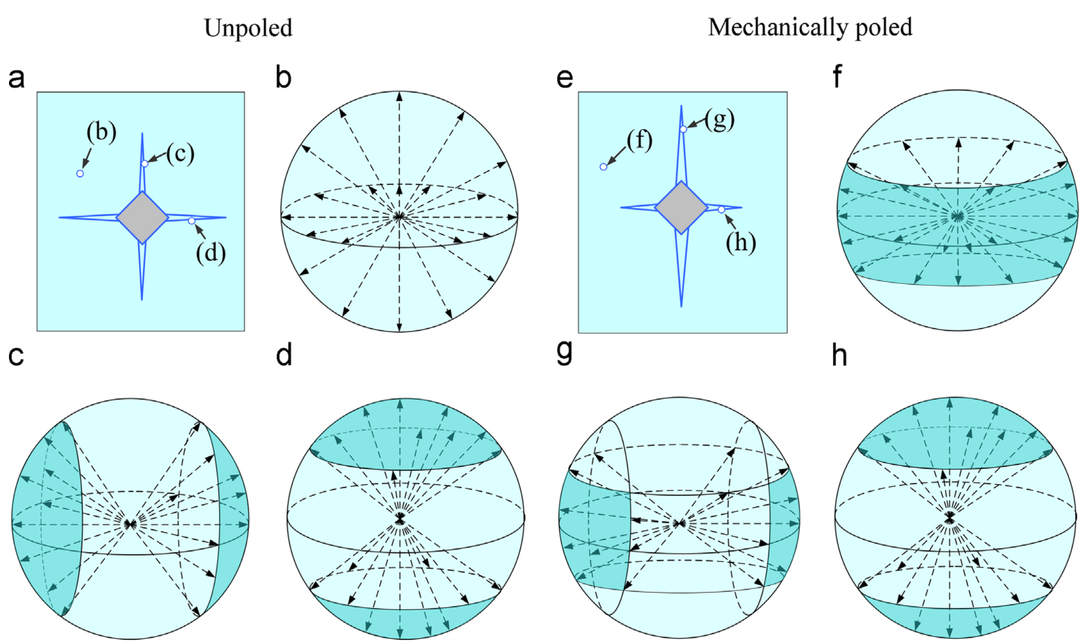


Fig. 9. Domain textures evolution near the crack surface during indentation on the unpoled (a)–(d) and mechanically poled (e)–(h) PZT samples.

respectively. The energy dissipated by these two types of domain switching is the same, i.e., the enhancement of the critical ERR ($\Delta G_{IC}$) is isotropic, leading to the isotropic fracture toughness in the unpoled ferroelectric ceramics. After mechanical poling, most domains switched to a state with their polar axes as perpendicular as possible to the loading direction, as shown in Fig. 9(f). Thus during indentation, more domains near the surfaces of the perpendicular crack can switch from Fig. 9(f) to (h), leading to a larger $\Delta G_{IC}$ during crack propagation. In comparison, the switchable domains from Fig. 9(f) to (g) become less near the parallel crack surface and $\Delta G_{IC}$ is small for the parallel crack. Hence, $K_{IC}^{\perp}$ is larger than $K_{IC}^{\parallel}$ for the MP samples, leading to the FTA behavior.

However, for the electrically poled specimen, the polar axes of most domains have been oriented by the strong poling field, as shown in Fig. 10(b). During Vickers indentation, the domain textures will evolve from Fig. 10(b) to (c) near the parallel crack surface; while the domain textures almost do not change near the perpendicular crack surface, i.e., little domain switching occurs from Fig. 10(b) to (d), leading to $K_{IC}^{\parallel} > K_{IC}^{\perp}$. After mechanical depoling by large stress (say 400 MPa), the domain textures turn to be very similar with that in the mechanically poled sample. Therefore, the fracture toughness in MD samples is also anisotropic with $K_{IC}^{\perp} > K_{IC}^{\parallel}$. When the applied stress is not enough to completely depole the sample, the domain textures will be at an intermediate axisymmetric state between Fig. 10(b) and (f) and $K_{IC}^{\parallel}$ can be larger, equal or smaller than $K_{IC}^{\perp}$, depending on the applied stress, as shown in Fig. 8(b).

The enhancement of critical ERR induced by domain switching can be estimated in a similar manner with Mehta et al. and Schneider et al. [14,25], by the following expression:

$$\Delta G_{IC} = 2h\sigma_{coercive}\varepsilon_{switch} \tag{3}$$

where $\sigma_{coercive}$ is the coercive stress; $\varepsilon_{switch}$ is the domain switching induced strain variations in the direction perpendicular to the crack surface; and $h$ is the height of the domain switching zone near the crack tip, as shown in Fig. 11. It should be pointed out that the domain switching zone induced by stress is much larger than that induced by the Lehovec effect during crack propagation [7,8,11]. Hence, we estimate the height of the domain switching zone by:

$$h = A(K_{IC}/\sigma_{coercive})^2 \tag{4}$$

where $A$ is a constant depending on the crack geometry and domain switching criterion. In addition, for brittle fracture, there is a relationship between the energy release rate and fracture toughness, i.e.,:

$$G_{Ic} = K_{Ic}^2/E' \tag{5}$$

where $E'$ equals $E(1-\upsilon^2)$ for the plane strain problem and it takes $E$ for the plane stress problems. Using Eqs. (2) and (5), we can build a relationship between the "intrinsic" fracture

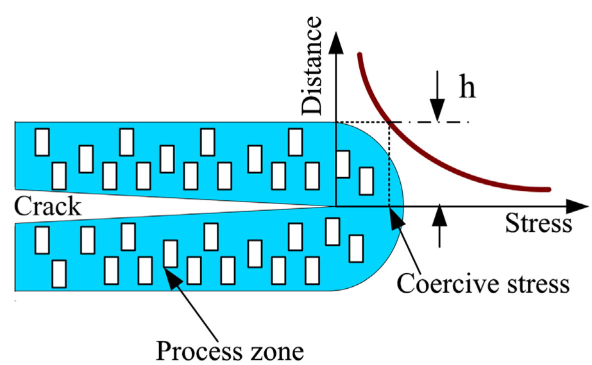


Fig. 11. Illustration of the domain switching zone in ferroelectric ceramics during crack propagation.

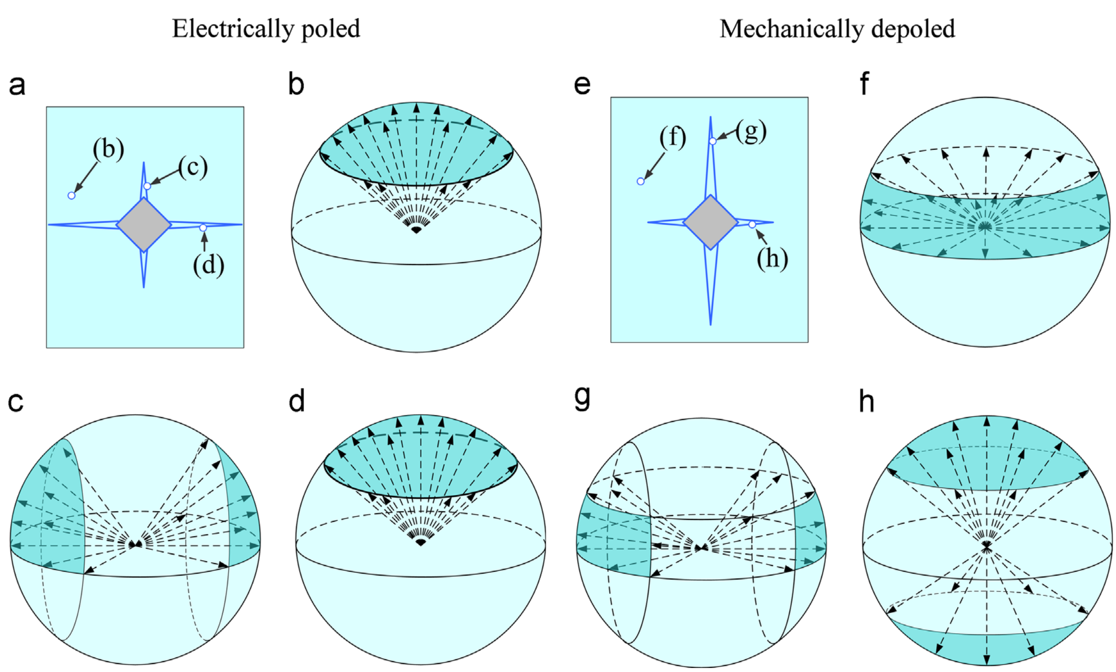


Fig. 10. Domain texture evolution near the crack surface during indentation on the electrically poled (a)–(d) and mechanically depoled (e)–(h) PZT samples.

toughness $K_0$ and the practical fracture toughness $K_{IC}$ as

$$K_{IC} = K_0 / \sqrt{1-\alpha\varepsilon_{switch}} \tag{6}$$

where $\alpha$ is a material constant which is the function of $E'$, $A$, and $\sigma_{coercive}$. From Eq. (6), it can be seen that the practical fracture toughness of ferroelectric material depends on both the "intrinsic" fracture toughness and the switchable strain near the crack surface.

If we further assume that: (i) $K_{IC}^{\perp}$ of the electrically poled sample is the "intrinsic" fracture toughness, i.e., no domain switching occurs during indentation near the perpendicular crack surface and (ii) for all the samples, the strain state beneath the crack surface is equivalent to the strain state after electric poling. Then the switchable strain beneath the crack surface during indentation for the MP and MD samples can be calculated by

$$\varepsilon_{Mpoled}^{\parallel} = \varepsilon_{Epoled}^{R} - \varepsilon_{Mpoled}^{R}/2 \tag{7a}$$

$$\varepsilon_{Mpoled}^{\perp} = \varepsilon_{Epoled}^{R} + \varepsilon_{Mpoled}^{R} \tag{7b}$$

$$\varepsilon_{Mdepoled}^{\perp} = \varepsilon_{Mdepoled}^{R} \tag{7c}$$

$$\varepsilon_{Mdepoled}^{\parallel} = 3\varepsilon_{Epoled}^{R}/2 - \varepsilon_{Mdepoled}^{R}/2 \tag{7d}$$

where $\varepsilon_{Mpoled}^{\parallel}$ and $\varepsilon_{Mpoled}^{\perp}$ are the switchable strains beneath the parallel crack surface and the perpendicular crack surface of the MP samples; $\varepsilon_{Mdepoled}^{\parallel}$ and $\varepsilon_{Mdepoled}^{\perp}$ are the switchable strain beneath the parallel crack surface and perpendicular crack surface of the MD samples; and $\varepsilon_{Epoled}^{R}$, $\varepsilon_{Mpoled}^{R}$, and $\varepsilon_{Mdepoled}^{R}$ are the remnant strains of the electrically poled, MP, and MD samples, which can be measured from strain curves during electric poling, mechanical poling and mechanical depoling, respectively. The calculated switchable strains are listed in Table 2, from which it can be seen that for both the MP and MD samples, with increasing compression, the switchable strain decrease beneath the parallel crack surface and increase beneath the perpendicular crack surface.

To show the validity of the proposed relationship between the fracture toughness and the switchable strain, i.e., Eq. (6), we plot both the experimental data and the theoretical curve in Fig. 12, where the parameter $\alpha$ in Eq. (6) was fitted using the measured data to be 1.48. It can be seen from Fig. 12 that most experimental data can be well described by the theoretical relationship in Eq. (6) although slight deviations still exist which may be caused by the grain boundary effect, reverse domain switching during crack propagation, etc.

It should be pointed out that the fracture behavior of the textured samples on the surface perpendicular to compression may also be influenced by domain reorientation during compression loading and should be isotropic. In fact, we have tried to measure the fracture toughness of textured specimen on the surface perpendicular to compression. However, it is very difficult to get credible results. That is because mechanical loading has to be conducted on bar shaped specimen to ensure the uniform stress distribution, while for the Vickers indentation measurement on the surfaces perpendicular to the compression, the bar shaped specimen cannot work and it has to be cut into plate-shaped

Table 2
The calculated switchable strains beneath the crack surface during crack propagation of the mechanically poled/depoled PZT samples.

| Compression stress (MPa) | Switchable strains beneath the crack surface (%) | | | |
|---|---|---|---|---|
| | Parallel (MP) | Perpendicular (MP) | Parallel (MD) | Perpendicular (MD) |
| 0 | 0.32 | 0.32 | 0.48 | 0 |
| 50 | 0.27 | 0.428 | 0.41 | 0.146 |
| 60 | – | – | 0.38 | 0.202 |
| 70 | – | – | 0.353 | 0.254 |
| 80 | – | – | 0.33 | 0.299 |
| 100 | 0.22 | 0.538 | 0.3 | 0.382 |
| 200 | 0.17 | 0.61 | 0.22 | 0.521 |
| 400 | 0.16 | 0.64 | 0.17 | 0.613 |

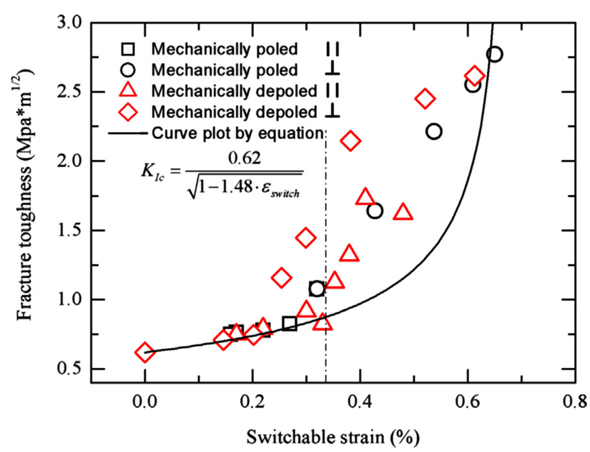


Fig. 12. Fracture toughness vs. switchable strain in the mechanically poled/depoled PZT sample.

samples. However, induced by the stresses or the heats generated during cutting, the domain texture on the new surface may considerably change. Fig. 13 shows the measured diffraction data on the new surface of a plate-shaped specimen cut from the 400 MPa mechanically poled sample. It can be seen that its $I_{002}^{T}/I_{200}^{T}$ ratio is larger than that of the unpoled specimen (for comparison, the diffraction data of the unpoled specimen is also plotted). However, during mechanical poling, it is known that the domains parallel to compression are depressed and that the $I_{002}^{T}/I_{200}^{T}$ ratio should decrease. This suggests that some domains reoriented parallel to the compression direction during cutting. Obviously, these reoriented domains will influence the fracture behavior on the surface perpendicular to compression. Therefore, the fracture toughness measured on such surface is incredible. Actually, some efforts are still ongoing aiming to conquer the above mentioned difficulties.

We also measured the dielectric constants of the mechanically poled PZT samples along the loading direction for different levels of compression, as shown in Fig. 14. It can be seen that below 100 MPa, the dielectric constant increases quickly with the applied compressive stress. Its increase slows down between 100 and 200 MPa, and the dielectric constant

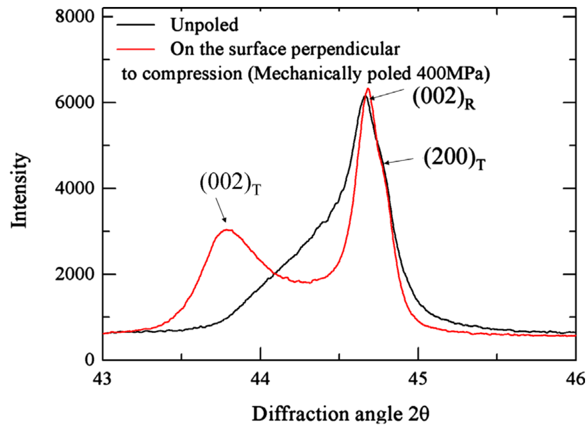


Fig. 13. X-ray diffraction results of a plate-shape specimen cut from the 400 MPa mechanically poled sample (on the surface perpendicular to compression).

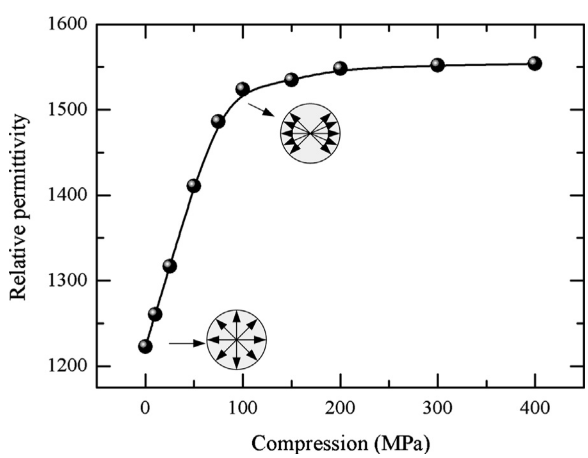


Fig. 14. Evolution of relative permittivity of PZT ceramics after mechanical poling with different levels of compression.

stabilized when the applied stress is higher than 200 MPa, which is consistent with the domain textures that is almost saturated at this stage. The dielectric constant of the fully mechanically poled (at 400 MPa) is 1550 in comparison of that of 1225 for the unpoled sample, with the total increase of 27%. Therefore, the mechanical poling could both increase the fracture toughness (within the plane perpendicular to the loading direction) and the dielectricity of the PZT samples. This conclusion should also apply for other ferroelectric ceramics such as $BaTiO_3$, which is very promising for enhancement of the performance and reliability of ferroelectric capacitors.

## 4. Conclusions

In summary, the fracture toughness of both the mechanically poled (MP) and the mechanically depoled (MD) PZT samples is systematically studied in this work. Results show that for both types of samples, the fracture toughness perpendicular to the loading direction ($K_{IC}^{\perp}$) increases and that parallel to the loading direction ($K_{IC}^{\parallel}$) decreases with increasing compressive stress. When the stress reaches its maximum of 400 MPa, $K_{IC}^{\perp}$ can reach 2.7 MPa $m^{1/2}$ and 2.6 MPa $m^{1/2}$ for the MP and MD samples, respectively. The fracture toughness anisotropy (FTA) ratio ($K_{IC}^{\perp}/K_{IC}^{\parallel}$) of the MP samples increases gradually from unity (unpoled sample) to 3.7 (400 MPa poled); while for the MD samples, the ratio $K_{IC}^{\perp}/K_{IC}^{\parallel}$ gradually increase from 1/2.6 (electrically poled sample) to 3.5 (400 MPa depoled). By analyzing the experimental results taking into account the domain switching toughening mechanism in ferroelectric ceramics, it is found that the variation of fracture toughness is caused by the domain texture-dependent switchable strain beneath the crack surface, i.e., the larger the switchable strain, the larger the fracture toughness. These obtained results could provide a useful guidance for improving the reliability and performance of ferroelectric capacitors.

## Acknowledgments

This work is supported by the Natural Science Foundation of China under Grant nos. 11002002 and 11090331.

## References

[1] B. Jaffe, W.R. Cook, H. Jaffe, Piezoelectric Ceramics, Academic, London/New York, 1971.
[2] K. Uchino, Piezoelectric Actuators and Ultrasonic Motors, Kluwer Academic, Boston, 1996.
[3] G.A. Schneider, Influence of electric field and mechanical stress on the fracture of ferroelectrics, Annual Review of Materials Research 37 (2007) 491–538.
[4] M. Kuna, Fracture mechanics of piezoelectric materials—where are we right now?, Engineering Fracture Mechanics 77 (2010) 309–326.
[5] F. Meschke, A. Kolleck, G.A. Schneider, R-curve behaviour of $BaTiO_3$ due induced ferroelastic domain switching, Journal of the European Ceramic Society 17 (1997) 1143–1149.
[6] S.L. dos Santos e Lucato, D.C. Lupascu, J. Rödel, Effect of poling direction on R-curve behavior in lead zirconate titanate, Journal of the American Ceramic Society 83 (2) (2000) 424–426.
[7] D.N. Fang, Y.J. Jiang, S. Li, C.T. Sun, Interactions between domain switching and crack propagation in poled $BaTiO_3$ single crystal under mechanical loading, Acta Materialia 55 (2007) 5758–5767.
[8] J.L. Jones, S.M. Motahari, M. Varioglu, U. Lienert, J.V. Bernier, M. Hoffman, E. Üstündag, Crack tip process zone domain switching in a soft lead zirconate titanate ceramic, Acta Materialia 55 (2007) 5538–5548.
[9] W. Yang, T. Zhu, Switch-toughening of ferroelectrics subject to electric fields, Journal of the Mechanics and Physics of Solids 46 (1998) 291–311.
[10] C.M. Landis, On the fracture toughness of ferroelastic materials, Journal of the Mechanics and Physics of Solids 51 (2003) 1347–1369.
[11] K.J. Lehovec, Space-charge layer and distribution of lattice defects at the surface of ionic crystals, Journal of Chemical Physics 21 (1953) 1123–1128.
[12] T. Yamamoto, H. Igarashi, K. Okazaki, Internal stress anisotropies induced by electric field in lanthanum modified $PbTiO_3$ ceramics, Ferroelectrics 50 (1983) 273–278.
[13] G.G. Pisarenko, V.M. Chushko, S.P. Kovalev, Anisotropy of fracture toughness of piezoelectric ceramics, Journal of the American Ceramic Society 68 (5) (1985) 259–265.
[14] K. Mehta, A.V. Virkar, Fracture mechanisms in ferroelectric–ferroelastic lead zirconate titanate (Zr:Ti=0.54:0.46) ceramics, Journal of the American Ceramic Society 73 (3) (1990) 567–574.

[15] F. Guiu, B.S. Hahn, H.L. Lee, M.J. Reece, Growth of indentation cracks in poled and unpoled PZT, Journal of the European Ceramic Society 17 (4) (1997) 505–512.

[16] J.M. Calderon-Moreno, M. Popa, Fracture toughness anisotropy by indentation and SEVNB on tetragonal PZT polycrystals, Materials Science and Engineering 319 (21) (2001) 692–696.

[17] F. Fang, W. Yang, Poling-enhanced fracture resistance of lead zirconate titanate ferroelectric ceramics, Materials Letters 46 (2000) 131–135.

[18] Y.W. Li, F.X. Li, Large anisotropy of fracture toughness in mechanically poled/depoled ferroelectric ceramics, Scripta Materialia 62 (2010) 313–316.

[19] S.C. Hwang, C.S. Lynch, R.M. McMeeking, Ferroelectrci/ferroelastic interactions and a polarization switching model, Acta Metallurgica et Materialia 43 (1995) 2073.

[20] F.X. Li, R.K.N.D. Rajapakse, A constrained domain-switching model for polycrystalline ferroelectric ceramics: Part I. Model formulation and application to tetragonal materials, Acta Materialia 55 (2007) 6472–6480.

[21] F.X. Li, R.K.N.D. Rajapakse, Analytical saturated domain orientation textures and electromechanical properties of ferroelectric ceramics due to electric/mechanical poling, Journal of Applied Physics 101 (2007) 054110.

[22] B. Noheda, J.A. Gonzalo, L.E. Cross, R. Guo, S.-E. Park, D.E. Cox, G. Shirane, Tetragonal-to-monoclinic phase transition in a ferroelectric perovskite: the structure of $PbZr_{0.52}Ti_{0.48}O_3$, Physical Review B 61 (13) (2000) 8687–8695.

[23] G.R. Anstis, P. Chantikul, B.R. Lawn, D.B. Marshall, A critical evaluation of indentation techniques for measuring fracture toughness: I. Direct crack measurements, Journal of the American Ceramic Society 64 (1981) 533.

[24] T. Fett, D. Munz, G. Thun, Young's modulus of soft PZT from partial unloading tests, Ferroelectrics 274 (2002) 67–81.

[25] G.A. Schneider, V. Heyer, Influence of the electric field on Vickers indentation crack growth in $BaTiO_3$, Journal of the European Ceramic Society 19 (1999) 1299–1306.